Structure and Reactivity of Platinum−Copper Alloy Particles Supported on ZSM-5

Efim S. Shpiro,[†] Olga P. Tkachenko,[†] Nils I. Jaeger,*[,‡] Günter Schulz-Ekloff,[‡] and Wolfgang Grünert[§]

Zelinsky Institute of Organic Chemistry, Moscow 117913, Russia; Institut für Angewandte und Physikalische Chemie, Universität Bremen, D-28334 Bremen, Germany; and Lehrstuhl für Technische Chemie, Ruhr-Universität Bochum, D-44780 Bochum, Germany

Received: February 5, 1998

Electronic and structural properties of highly dispersed Pt−Cu alloys supported on zeolite HZSM-5 with narrow particle size distribution (1−2 nm) were studied by transmission electron microscopy, X-ray photoelectron spectroscopy, and Fourier transform infrared spectroscopy of chemisorbed carbon monoxide. FTIR of adsorbed CO proved to be the most sensitive tool for the detection of alloy formation. Dilution of the platinum surface with copper can be recognized by the absence of dipole−dipole interaction between the chemisorbed CO molecules (geometric effect). A strong red shift of the vibration frequency of linearly bonded CO in conjunction with an increase of the relative intensity of bridge-bonded CO is discussed in terms of an electronic effect. All spectroscopic methods demonstrate the ready reoxidation and redispersion of the copper component of the particles and the reversible formation of the alloy again by repeated reduction.

1. Introduction

Platinum−copper alloys have been frequently investigated to elucidate the alloying effects in adsorption and catalysis.[1−6] The dilution of Pt with copper was found to be the main reason of the changes in catalytic activity and selectivity in such reactions as hydrogenation,[7] isomerization,[8] and hydrocracking.[9] Possible ligand effects caused by alloying remained rather obscure although shifts of the IR frequencies of adsorbed CO[10−14] and XPS chemical shifts have been found for Pt−Cu supported catalysts.[15,16] A special case of Pt−Cu systems is zeolite-hosted Pt−Cu alloys. It was demonstrated by Sachtler et al. for Pt−Cu in zeolite Y that the composition of the alloy particles and surface enrichment by either component strongly depend on the location of the metal precursors and the resultant metal particles in the various zeolite cages.[17,18] An unusual effect of Cu leaching from the alloy was found to occur due to the reoxidation of copper atoms by zeolite protons.[17] The structure and chemistry of monometallic ZSM-5-supported platinum and copper systems has been extensively studied in recent years with particular emphasis on the selective catalytic reduction of nitrogen oxides.[19−26] Highly dispersed platinum particles encapsulated in ZSM-5 have been identified at high temperatures.[27−29] By contrast, reduced copper easily aggregates on the external surface of ZSM-5 zeolite, as has been recently documented.[30,31]

In the present study electron microscopy and photoemission techniques have been combined with an IR study of adsorbed CO to investigate the conditions for the formation of bimetallic particles as well as their electronic and structural properties. The methods have been demonstrated earlier to be very efficient to elucidate the structure of Pt−Cr alloy particles in the ZSM-5 zeolite.[29]

2. Experimental Section

2.1. Materials. Platinum−copper catalysts were prepared by ion exchange followed by impregnation of H−ZSM-5 zeolite (Si/Al = 16.5). The starting material was prepared by thermal decomposition of the NH_4−ZSM-5. The metals were introduced from <0.01 M aqueous solutions of $Pt(NH_3)_4Cl_2$ and $Cu(NO_3)_2$ in successive steps. The solutions contained the total amount of the metal to be inserted. The first step of conventional ion exchange by stirring the zeolite with the solution for several hours was followed by evaporation of the solvent in order to deposit the remaining metal not ion exchanged onto the support. Following the introduction of the first element (Pt), the material was calcined in air up to a final temperature of 773 K using a temperature program reported earlier, thus completing the ion exchange in a solid-state process.[32] This procedure was repeated after the loading of the sample with the second component (Cu). All samples contain 1% Pt, together with 2% Cu (atomic ratio Cu/Pt = 6, theoretical total exchange degree 70%, sample 1), 0.6% Cu (Cu/Pt = 2, theoretical total exchange degree 30%, sample 2), and 0.3% Cu (Cu/Pt = 1, theoretical total exchange degree 20%, sample 3). The catalysts were then reduced in flowing hydrogen under conditions reported below either in-situ in the cell of the FTIR spectrometer or in the preparation chamber of the XPS spectrometer.

2.2. XPS. Electron emission spectra were obtained with a Kratos XSAM 800 spectrometer using Mg Kα and Al Kα radiation. The experimental procedures were described in detail elsewhere.[33] The binding energy (BE) scale was calibrated with the C 1s and Si 2p lines (BE = 285.0 and 103.4 eV, respectively). To minimize a possible reduction of Cu^{2+} in the precalcined samples by X-ray irradiation, the samples were cooled to 190 K during the measurements. Nevertheless, a partial reduction of Cu^{2+} was noted by a decreasing intensity of the Cu 2p shake-up satellite during data acquisition. Since the Pt 4f spectra were partially overlapped by the Al 2p and Cu 3p lines, the parameters of Pt $4f_{7/2}$ were determined using a peak synthesis procedure. The surface atomic ratios were estimated by usual procedures as described elsewhere.[33] Analyzer transmission factors were determined by calculating the intensity ratios for different lines of the pure metals (Cu, Au, Pt).

* To whom correspondence should be addressed.
[†] Zelinsky Institute of Organic Chemistry.
[‡] Universität Bremen.
[§] Ruhr-Universität Bochum.

S1089-5647(98)01029-3 CCC: $15.00
Published on Web 04/18/1998

TABLE 1: Parameters of XPS Spectra and Surface Atomic Ratios for 1% Pt−2% Cu/H−ZSM-5

	BE, eV		KE Cu L_3VV, eV		Cu Auger parameter, eV		atomic ratios		
	Pt $4f_{7/2}$	Cu $2p_{3/2}$	1	2	1	2	Cu/Si × 10^3	Pt/Si × 10^3	Cu/Pt[a]
initial	74.7	933.1[b]	912.8		1845.9		14	1.8	7
H_2, 493 K	71.0	932.1	914.4	918.2	1846.5	1850.3	15	1.1	15
H_2, 523 K	71.0	932.4	913.8	918.2	1845.9	1850.3	13	1.1	13
H_2, 623 K	71.1	932.0		918.6			11	1.1	11

[a] Bulk Cu/Pt ratio: 6.0 (by AAS). [b] Weak intensity of shake-up satellite is explained by Cu^{2+} autoreduction during spectra acquisition.

2.3. FTIR and TEM. Infrared spectra were recorded with a Bio-Rad FTS 60A single-beam FTIR spectrometer in the range 400−4000 cm^{-1} with a resolution of 2 cm^{-1}. The catalysts were pressed into thin wafers (4−6 mg/cm^2) and mounted in an in-situ cell.[29] Before spectra collection, the samples were evacuated and reduced in static hydrogen at 10^3 Pa at appropriate temperatures. In addition, some of the specimens were reoxidized in O_2 directly in the cell. After the treatments, background spectra were recorded in the absence of CO at different temperatures. In a first series of runs, the samples were exposed to flowing CO at $\approx 10^{-1}$ Pa, and spectra were taken at 300 K both in CO and after evacuation. In a second series, the samples were subjected to 4×10^3 Pa of CO in static mode, and spectra were recorded in the presence of gaseous CO, during slow evacuation through a capillary, and after rapid evacuation. After evacuation at ambient temperature, the remaining adsorbates were desorbed at $\approx 10^{-4}$ Pa by linearly increasing the temperature (5 K/min). During the temperature program spectra were recorded at selected temperature levels.

Following the reduction of the samples at 523 and 623 K, reoxidation at 523 K and again after recovering the zeolite wafers from the IR cell the material was investigated by TEM as described earlier.[29] The size of around 95% of the metal particles was found to be in the range 1−2 nm rather uniformly distributed over the imaged area of the supporting zeolite crystal without any accumulation at the edges of the specimens. In addition, larger aggregates (5−10 nm) could be observed, the relative fraction of which was higher in the samples reduced at 623 K.

3. Results

3.1. XPS. XPS data for a representative sample (sample 1) are summarized in Table 1. Owing to the partial reduction of Cu^{2+} to Cu^+ under X-ray irradiation, the Cu $2p_{3/2}$ BE of the initial sample represents a mixture of two oxidation states. It should be noted, however, that the Cu L_3VV kinetic Auger energies are characteristic of copper cations located inside zeolite channels (KE ≈ 913 eV).[19]

Both platinum and copper are reduced to the metallic state in the first treatment with hydrogen at 493 K. In the Cu Auger spectra, a component remaining at low KE may indicate, however, that the reduction was not complete or that very small intrazeolite Cu particles have been formed in addition to the bulk copper.[19] At higher temperatures (623 K), only the peak characteristic of a metallic bulklike copper phase was observed in the Cu L_3VV spectra. The Pt $4f_{7/2}$ peak has a binding energy close to that of the bulk metal (71.0−71.1 eV). Only in the initial sample, the Cu/Pt atomic ratio near the external surface was close to that in the bulk while surface enrichment with copper was found for the reduced samples.

3.2. FTIR. *3.2.1. Calcined Samples.* Figure 1 shows the IR bands of CO adsorbed on the calcined sample 1 (1% Pt−2% Cu) after CO adsorption at 4×10^3 Pa in the presence of the gas-phase CO (spectrum 1) and after removal of the gas phase under different evacuation regimes. After CO adsorption, two strong bands at 2150 and 2177 cm^{-1} were observed along with

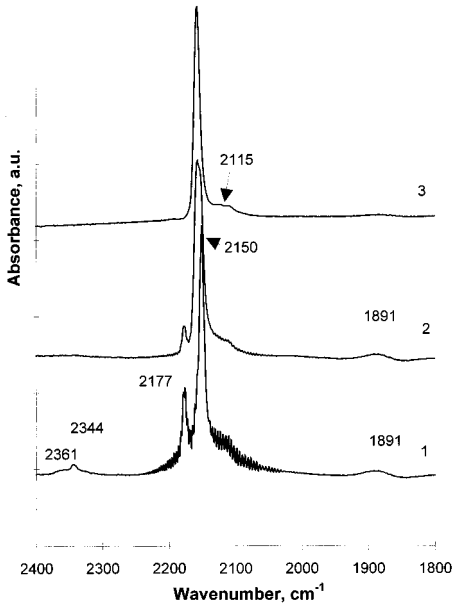

Figure 1. FTIR spectra of adsorbed CO at 300 K over calcined 1% Pt−2% Cu/ZSM-5 sample: 1, 60 min adsorption (4×10^3 Pa); 2, 30 min desorption (slow evacuation); 3, 60 min fast evacuation.

a shoulder at 2115 cm^{-1}, which is masked by rotation modes of gas-phase CO, and a weak band at 1891 cm^{-1}. CO evacuation results in a decrease of the band at 2177 cm^{-1} and a shift of the band at 2150 cm^{-1} to 2157 cm^{-1} (spectrum 2). After the sample was pumped off to 10^{-4} Pa, the narrow band at 2157 cm^{-1} and a shoulder at 2115 cm^{-1} remained in spectrum 3. The band at 2150 cm^{-1} and the band at 2157 cm^{-1} can be assigned to CO adsorbed on Cu^+ sites.[30,31]

With the exception of the shoulder at 2115 cm^{-1}, these typical features could be observed in all calcined samples; additional bands appeared for samples with lower Cu contents.

The exposure of the calcined sample 2 (*1% Pt−0.6% Cu)* to CO at low pressure (10^{-1} Pa, Figure 2, spectrum 1) results in two bands at 2157 and 2092 cm^{-1}. At high pressure (4×10^3 Pa), the band at 2157 cm^{-1} was found to increase, and an additonal band appeared at 2179 cm^{-1} (Figure 2, spectrum 3). Upon evacuation at 300 K the band at 2179 cm^{-1} could be easily removed while no significant changes are noted for the remaining bands in neither peak position nor intensity (spectra 4 and 5).

For sample 3 (*1% Pt−0.3% Cu)* upon low-pressure exposure to CO bands at 2157, 2126, and 1886 cm^{-1} were observed (Figure 3, spectrum 1). At elevated CO pressure (spectrum 2), the same bands at 2177 cm^{-1}, 2150 cm^{-1}, and shoulder at 2126 cm^{-1} were found while slow pumping resulted in a better spectral resolution (spectrum 3): some bands near the central peak at 2150−2157 cm^{-1}, which were present only as shoulders in the previous spectrum, are now well resolved. They are located at 2200, 2177, and 2128 cm^{-1}. The bands at 2200 and 2126 cm^{-1} can be assigned to CO linearly bonded to Pt^{2+} and to $Pt^{\delta+}$, respectively (Table 2 and references therein).

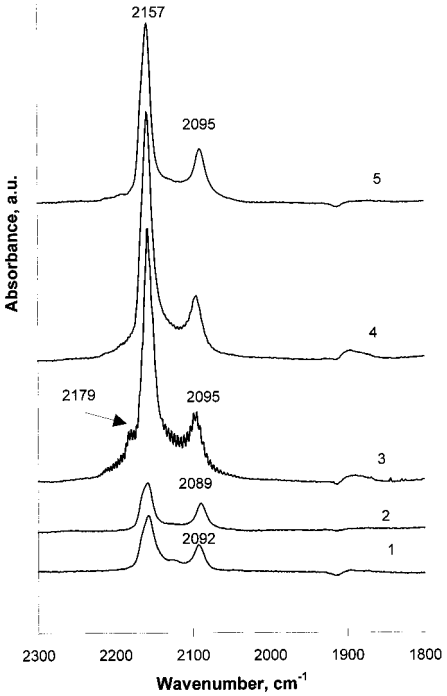

Figure 2. FTIR spectra of adsorbed CO at 300 K over calcined 1% Pt−0.6% Cu/ZSM-5 sample: 1, 10 min adsorption (ca. 10^{-1} Pa); 2, 30 min desorption; 3, 30 min adsorption (4×10^3 Pa); 4, 30 min (slow); 5, 30 min (fast) evacuation.

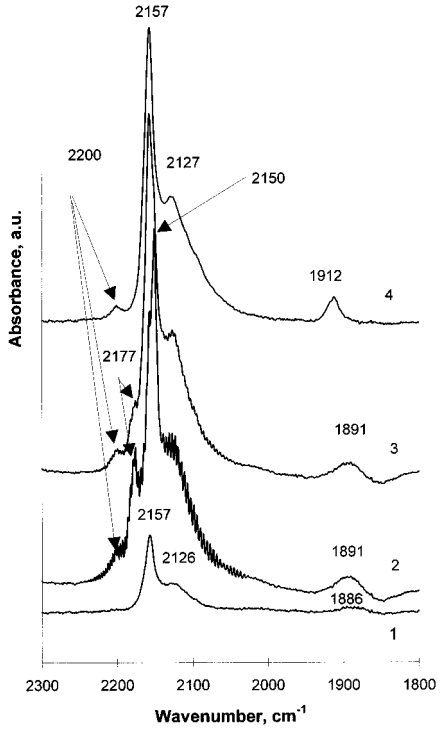

Figure 3. FTIR spectra of adsorbed CO at 300 K over calcined 1% Pt−0.3% Cu/ZSM-5 sample: 1, 30 min adsorption (ca. 10^{-1} Pa); 2, 30 min adsorption (4×10^3 Pa); 3, 30 min desorption (slow evacuation); 4, 30 min (fast evacuation).

3.2.2. Samples Reduced at 523 and 623 K. The spectral changes observed after adsorption, evacuation, and thermodesorption of CO for sample 1 reduced in hydrogen at 523 K are shown in Figure 4. Short exposure to CO at ambient temperature (20 s, 4×10^3 Pa of CO) gives rise to bands centered at 2150, 2024 (weak), and 1890 cm^{-1}. After 60 min exposure to CO (spectrum 1), bands were observed at 2150, 2177, and 1889 cm^{-1}; the band at 2024 cm^{-1} increased in intensity and shifted

TABLE 2: Frequencies Observed on Calcined and Reduced Pt−Cu/HZSM-5 Catalysts and Assignment

freq (cm^{-1})	assignt	comment	ref
2200	Pt^{2+}−CO		39
2177	$Cu^{+}(CO)_2$	symmetric vibration	40
2150	$Cu^{+}(CO)_2$	asymmetric vibration	40 and refs therein
2157	Cu^{+}−CO		40, 42, 43
2115	$Cu^{+}-{}^{13}CO$		40
2126	Pt^{0}−CO	Pt atoms	10
2095	$Pt^{\delta+}$−CO	cluster	41
2086	Pt^{0}−CO	cluster, 1−3 nm	29
2060−2066	Pt^{0}−CO	Pt/Cu alloy cluster 1−2 nm	this work
2048−2041	Pt^{0}−CO	Pt/Cu alloy enriched in Cu cluster 1−2 nm	this work

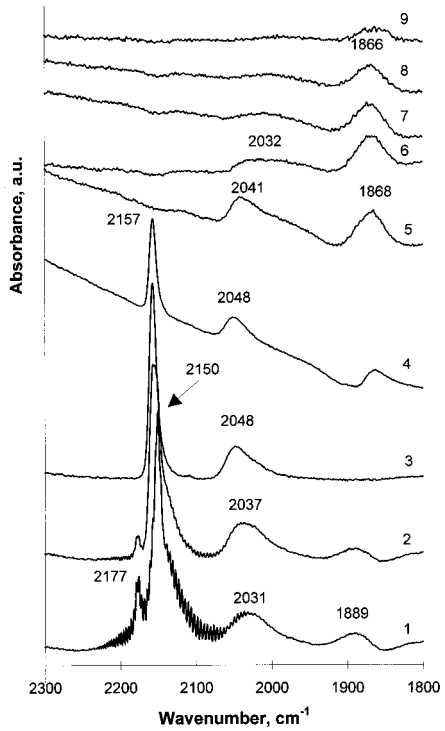

Figure 4. FTIR spectra of adsorbed CO at 300 K over low-temperature reduced (523 K) 1% Pt−2% Cu/ZSM-5 sample: 1, 60 min adsorption (4×10^3 Pa); 2, 30 min slow evacuation; 3, 1 min fast evacuation; 4, 323 K; 5, 423 K; 6, 473 K; 7, 523 K; 8, 573 K; 9, 623 K thermodesorption.

to 2031 cm^{-1}. Slow and fast evacuation of the gas phase (spectra 2 and 3, respectively) resulted in a decrease and, finally, in a complete removal of the bands at 2177 and 1890 cm^{-1}. It was accompanied by the formation of the narrow band at 2157 cm^{-1} and a gradual shift of the band at 2031 cm^{-1} to 2048 cm^{-1}. Upon thermodesorption the band at 2157 cm^{-1} decreased and abruptly vanished when the temperature reached 423 K (spectrum 5), while the band at 2048 cm^{-1} was shifted to 2033 cm^{-1} and strongly decreased between 423 and 523 K (spectra 5−7). By contrast, the band at 1889 cm^{-1} increased and shifted to 1866 cm^{-1} (spectra 8 and 9). Bands in the ranges 2000−2100 and 1800−1900 cm^{-1} can be assigned to CO linearly and bridged adsorbed on Pt^0 crystallites.[27,29]

The FTIR spectra of the specimen reduced at 623 K and exposed to CO at 300 K (Figure 5) are rather similar to those observed previously (Figure 4) with the exception of the band at ca. 1880 cm^{-1}. The intensity of this band as compared to the remaining ones is higher than in the previous sample, and upon evacuation at room temperature it remains in the spectrum (spectrum 3). Upon thermodesorption, CO is first removed from the Cu sites (spectra 4−6) while bridged CO on Pt ("narrower" component) is very stable. It should be noted that the bands of

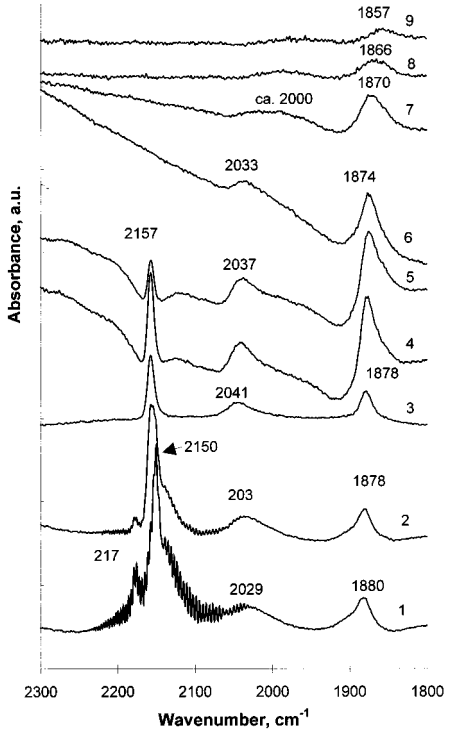

Figure 5. FTIR spectra of adsorbed CO at 300 K over high-temperature reduced (623 K) 1% Pt−2% Cu/ZSM-5 sample: 1, 60 min adsorption (4×10^3 Pa); 2, 30 min slow evacuation; 3, 60 min fast evacuation; 4, 323 K; 5, 373 K; 6, 423 K; 7, 473 K; 8, 573 K; 9, 623 K thermodesorption.

both linear and bridged CO exhibit considerable shifts to lower wavenumbers. The resulting weak bands observed at 473−623 K are located at ca. 2000 cm^{-1} (spectrum 7) and 1870−1857 cm^{-1} (spectra 7−9).

For sample 2 (1% Pt−0.6% Cu) reduced at 523 K, the band of Pt−CO appears at 2054 cm^{-1} and shifts to 2069 cm^{-1} under elevated CO pressure (Figure 6a, spectra 1 and 2). Evacuation at 300 K gradually removes the band at 2178−2182 cm^{-1}, which was observed at higher CO pressure (spectra 3 and 4). At higher evacuation temperatures, CO on Cu^+ (2157 cm^{-1}) is pumped off. The band of Pt−CO slightly decreases and shifts from 2066 cm^{-1} following evacuation to 2052 cm^{-1} at 473 K and 2049 cm^{-1} at 523 K (Figure 6b, spectra 1−6).

In the case of sample 2 reduced at 623 K a band at 2055 cm^{-1} (exposure to low CO pressure, spectrum 1) and at 2064 cm^{-1} (exposure to high CO pressure, spectrum 3) can be observed (Figure 7a). Upon evacuation and thermodesorption, this band shifts from 2060 cm^{-1} at 300 K to 2038 cm^{-1} at 523 K (Figure 7b, spectra 2−6) and vanishes from the spectrum at 573 K.

Following the reduction of the sample with the lowest Cu content (sample 3, 1% Pt−0.3% Cu) at 523 K two strong bands at 2158 and 2064 cm^{-1} were observed at low CO pressure. The intensity of the latter band does not change during evacuation at room temperature. Upon thermodesorption up to 473 K the band of Pt−CO is shifted by only 9 cm^{-1}.[34]

Oxidation and rereduction of the sample at 623 K gives spectra which, at first glance, look rather similar to those observed for the sample reduced at 523 K, i.e., two principal bands of Cu^+−CO and Pt−CO at 2157 and 2068 cm^{-1}, respectively (Figure 8). High-pressure adsorption gives a better resolved structure around the band at 2157 cm^{-1} while the band at 2072 cm^{-1} became even broader and more asymmetrical (spectrum 2). The bands at 2224 and 2181 cm^{-1} represent sites

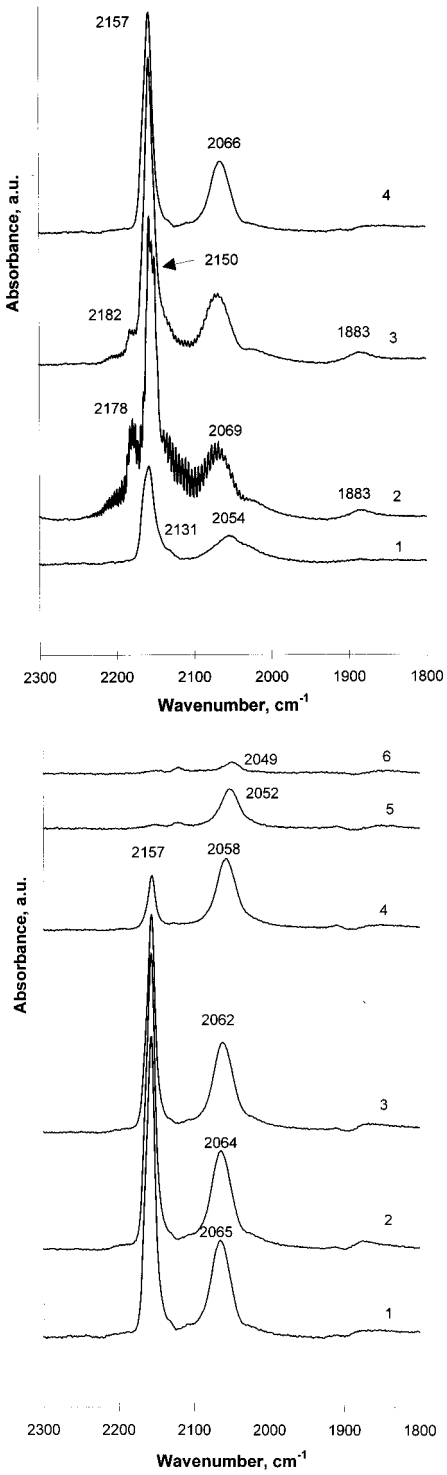

Figure 6. FTIR spectra of adsorbed CO at 300 K over low-temperature reduced (523 K) 1% Pt−0.6% Cu/ZSM-5 sample: (a) 1, 30 min adsorption (ca. 10^{-1} Pa); 2, 30 min adsorption (4×10^3 Pa); 3, 30 min (slow); 4, 30 min (fast) evacuation; (b) 1, 300 K; 2, 323 K; 3, 373 K; 4, 423 K; 5, 473 K; 6, 523 K thermodesorption.

of weak CO adsorption which are removed upon evacuation at room temperature (spectra 3 and 4). The principal bands at 2157 and 2068 cm^{-1} gradually decreased upon thermodesorption (cf. ref 34). The Cu^+−CO band was shifted very slightly and vanished at 473 K while the Pt−CO band underwent a downward shift of 30 cm^{-1} and remained in the spectrum still at 623 K.

3.2.3. Reoxidation of Reduced Samples. Treatment of the reduced samples in oxygen at 523 K results in spectra

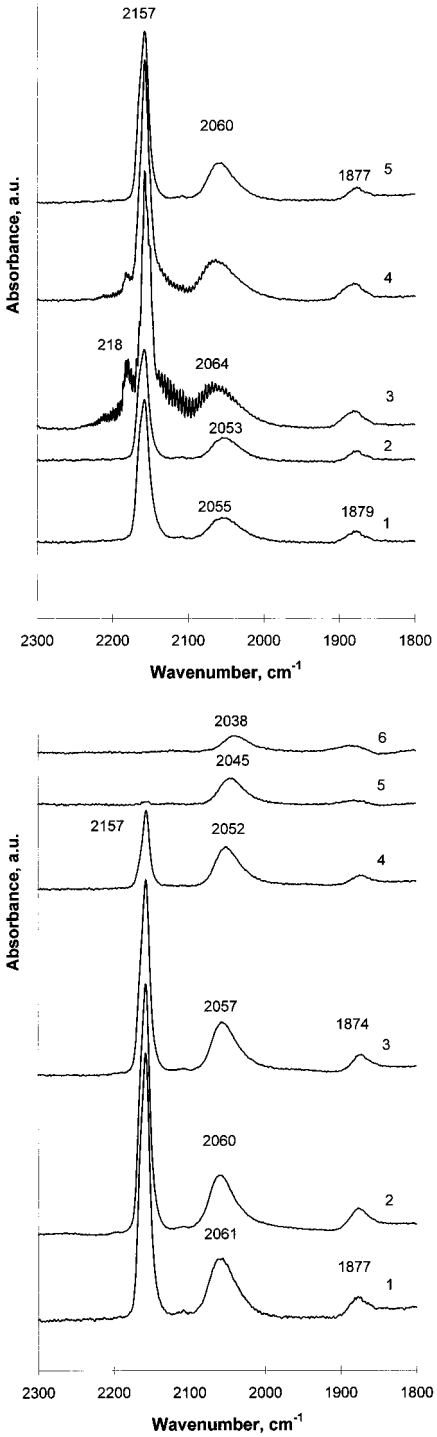

Figure 7. FTIR spectra of adsorbed CO at 300 K over high-temperature (623 K) reduced 1% Pt-0.6% Cu/ZSM-5 sample: (a) 1, 30 min adsorption (ca. 10^{-1} Pa); 2, 30 min desorption; 3, 30 min adsorption (4×10^3 Pa); 4, 30 min (slow); 5, 60 min (fast) evacuation; (b) 1, 300 K; 2, 323 K; 3, 373 K; 4, 423 K; 5, 473 K; 6, 523 K thermodesorption.

resembling those of the initial calcined sample with respect to the adsorption of CO on Cu. A typical example is depicted for sample 2 in Figure 9a which has to be compared with Figure 2 (sample 2, calcined). Upon desorption at increasing temperatures (Figure 9b), the band of Cu^+-CO vanishes at 523 K. The band of Pt−CO at 2086 cm^{-1} remains in the spectrum and was found to decrease and shift to lower wavenumbers in the temperature range 300−523 K (spectra 1−6) by about 25 cm^{-1} until it disappears beyond 573 K.

Oxygen treatment of the reduced sample 3 (1% Pt−0.3% Cu) at 523 K led to FTIR spectra with only one band at 2091 cm^{-1}

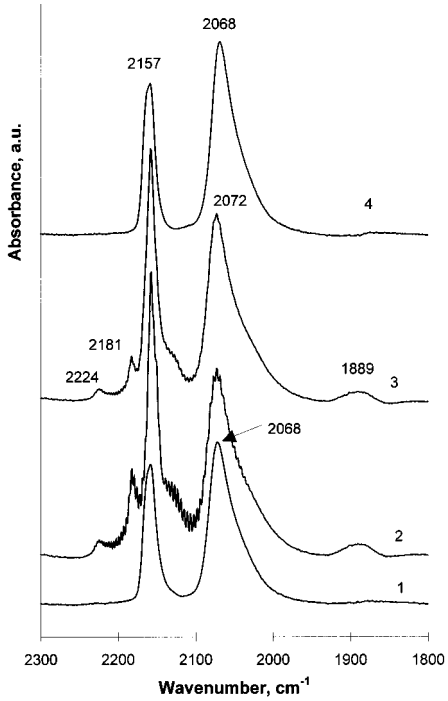

Figure 8. FTIR spectra of adsorbed CO at 300 K following reduction (523 K), reoxidation (523 K), and high-temperature reduction (623 K) of the 1% Pt−0.3% Cu/ZSM-5 sample: 1, 30 min (ca. 10^{-1} Pa); 2, 30 min (4×10^3 Pa) exposure; 3, 30 min (slow); 4, 30 min (fast) evacuation.

at low CO pressure. At elevated pressure bands at 2157 and 1888 cm^{-1} also developed. CO evacuation at ambient temperature had no pronounced effect on these two bands. The most pronounced change upon thermodesorption was the large downward shift of the Pt−CO band from 2088 cm^{-1} at 300 K to 2062 cm^{-1} at 523 K (cf. ref 34). On the other hand, the intensity decrease in this temperature region was only 2-fold. The band at 2157 cm^{-1} disappeared completely at 423 K.

4. Discussion

4.1. TEM Results. The TEM results given in the Experimental Section, the high aluminum content of the ZSM-5 zeolite, and the relatively low total degree of ion exchange allow the conclusion that the highly dispersed metal is located within the framework of the supporting zeolite. This is of relevance to the following discussion of the XPS and the FTIR results. Only a small number of large aggregates of 5−10 nm size have been found on the external surface. Their contribution was more significant after reduction at 623 K. The results agree with the estimation of the particle sizes on the basis of EXAFS coordination numbers.[35] The suppression of the surface dynamics of small metal particles encaged within a zeolite matrix[36] may be the reason for the agreement. Thermal movement of atoms can lead to an underestimate of the coordination number as has been pointed out by Clausen et al.[37]

The dimension of the intrazeolite metal particles exceeds the diameters of the voids in the ZSM-5 structure. The growth of metal crystals exceeding the dimensions of available cages, channels, and intersections starting at defects and leading to the local fragmentation of the surrounding lattice has been investigated in detail and reported repeatedly namely in the case of faujasites.[38] A size limiting factor appears to be the aluminum content of the zeolite. Proof came from a correlation of TEM results with XPS, ^{29}Si NMR spectroscopy, and the evaluation of adsorption isotherms. The latter method revealed the formation of mesopores around the metal particles.

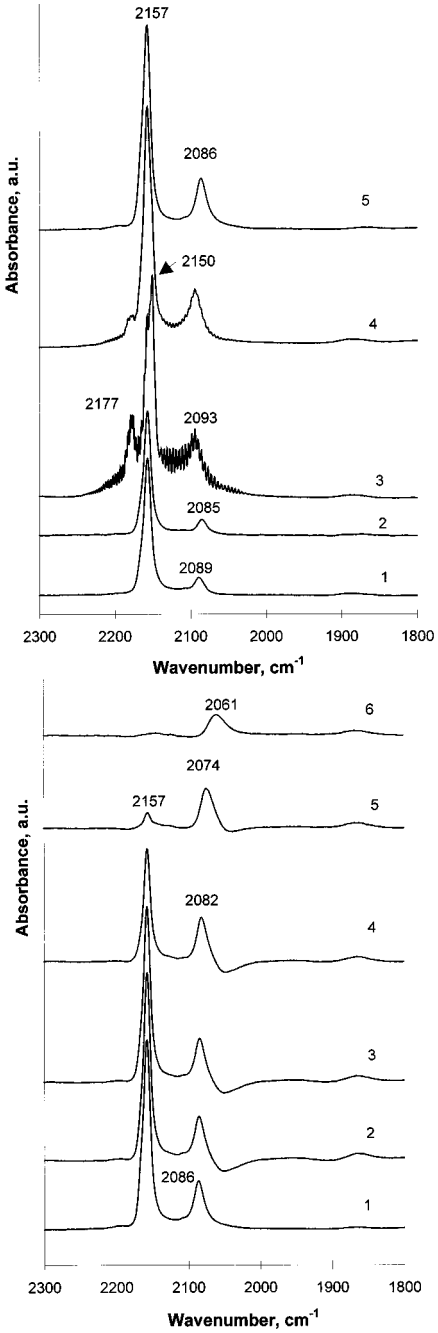

Figure 9. FTIR spectra of adsorbed CO at 300 K over reoxidized (523 K) 1% Pt−0.6% Cu/ZSM-5 sample: (a) 1, 30 min adsorption (ca. 10^{-1} Pa); 2, 30 min desorption; 3, 30 min adsorption (4×10^3 Pa); 4, 30 min (slow); 5, 60 min (fast) evacuation; (b) 1, 300 K; 2, 323 K; 3, 373 K; 4, 423 K; 5, 473 K; 6, 523 K thermodesorption.

4.2. XPS Data. The dependence of the Cu Auger parameter on the copper dispersion and location was amply applied and confirmed in our previous study on the monometallic Cu−ZSM-5 system.[19] It was found that small Cu^0 clusters resemble Cu^+ ions in their relaxation properties yielding very low values of the kinetic Auger energy and the Auger parameter. Larger Cu particles aggregated on the external zeolite surface exhibited Auger characteristics close to those of the bulk metal. From the BE, KE, and copper Auger parameters in the calcined sample 1 (Table 1, entry 1) follows that copper is present as Cu^{2+} inside the channels of the H−ZSM-5, as was found previously for the exclusively copper-loaded zeolite.[19] Reduction of this sample at 493 and 523 K produces Cu species in different environments; i.e., part of the copper is located on the external surface of the zeolite carrier crystals as large aggregates while the Auger parameter of the remaining copper coincides with that of intrazeolite Cu^+ or very small Cu^0 clusters.[19] However, TPR data not included in this paper show that both Cu and Pt are completely reduced already at 423 K in this sample, and the EXAFS results confirm the complete copper reduction as no significant Cu−O distance contribution was observed.[35]

This is not in contradiction to the FTIR results, which show the presence of Cu^+ in all spectra of the reduced samples regardless of the reduction temperature. After removal of H_2 the small Cu metal clusters identified by their Auger parameter will be reoxidized by Broensted acid sites available within the zeolite in the presence of CO as has been shown by Sachtler et al.[30]

After reduction at 623 K, only one Auger transition characteristic of bulk copper particles was found while the IR spectra of adsorbed CO still exhibit the Cu^+-derived bands, which are assigned above to species resulting from the reoxidation of small Cu metal clusters. It should, however, be noted that XPS and XAES are surface-sensitive methods while FTIR probes the material in total. At 523 K, where the segregation tendency of the Cu metal was low, the small clusters were still observed by the surface-sensitive techniques. At 623 K the segregation tendency is markedly increased (viz. TEM), and it is quite plausible that this affects the regions near the external surface first. While these are depleted of clusters, the bulk may well contain small Cu clusters even after reduction at 623 K.

A question arises as to the relaxation properties of Cu in the Pt−Cu alloy particles of ca. 2 nm size. Pt−Cu bonds have been detected by EXAFS even after reduction at 753 K;[35] i.e., the alloying strongly suppresses the segregation tendency of the copper.

Hence, Pt−Cu particles should be stable also in the regions near the external surface. There is, however, only the Auger transition typical of bulk Cu metal at reduction temperatures <623 K. Obviously, the relaxation behavior of the Cu metal in the alloy particles resembles that typical for the monometallic crystallites. Pt/Cu belongs to the weakly exothermic alloys; i.e., bonding is weak, and individual components preserve their identity.[11] This question certainly deserves further investigation.

4.3. FTIR Spectra. The observed bands, their assignments, and the corresponding references are summarized in Table 2.

4.3.1. Calcined and Reoxidized Samples. The strongest band in all calcined samples (Figures 1−3) as well as in the reoxidized sample 2 (Figure 9) is a narrow singlet at 2157 cm^{-1}. It appears upon evacuation of the samples exposed to CO and can be assigned to the Cu^+ monocarbonyl which is well documented in several studies.[30,31,40,42,43] The presence of Cu^+ is a result of the reduction of copper oxide species by CO.[31,40] This is most clearly seen in sample 1 with the highest Cu loading. The band due to CO_2 around 2350 cm^{-1} can be observed in the spectra. It is depicted as an example in Figure 1 (spectrum 1). Upon exposure to CO at elevated pressure even the dicarbonyl can be identified by the bands at 2177 and 2150 cm^{-1}. This assignment was proven by isotope exchange combined with force field calculations.[40] Actually, the latter consists of two separate narrow bands (fwhm = 9−11 cm^{-1}), the observation of which is dependent upon the CO pressure. Evacuation leaves the band at 2157 cm^{-1} characteristic for the Cu^+ monocarbonyl. The shoulder at 2115 cm^{-1} is due to the natural abundance of ^{13}CO.[40] Assignment of the band at 2177 cm^{-1} to CO attached to true zeolitic Lewis acid sites[31] can be ruled out since the band cannot be observed for Pt−HZSM-5 under the same experimental conditions.[29]

The low-temperature water gas shift reaction can be expected to lead to a partial reduction of platinum ions[44] depending on their accessibility in the zeolite support. A band at around 1891 cm^{-1} which appears in all calcined samples can be assigned to CO bridge-bonded to Pt. The samples with the relative highest Pt loading show the more pronounced indications of reduced Pt; i.e., the band at 2095 cm^{-1} (sample 2, Figure 2) can be assigned to CO atop bonded to $Pt^{\delta+}$.[41]

Following Zholobenko et al.,[10] the band at 2126 cm^{-1} (Figure 3, sample 3) can be assigned to monatomic Pt^0 particles. The band can be detected in Pt−ZSM-5 only under conditions of mild reduction of samples with low Pt content.[45] A high copper content might prevent the dispersion of the Pt atoms due to agglomeration centers provided by the copper ions.

Platinum oxide particles if present could be reduced by CO, and as a consequence the band could also be assigned to PtO.[41] In this case the band could be expected to appear in samples 1 and 2 with the higher copper content as well, which is not the case. The proposed assignment requires the presence of isolated Pt^{2+} ions which is likely the case under the calcination conditions. Mild reduction conditions are provided by the low-temperature water gas shift reaction.

The band at 2086 cm^{-1} in the reoxidized sample 2 (Figure 9) and at 2091 cm^{-1} in the reoxidized sample 3 is typical for atop bonded CO to Pt^0. Upon thermal desorption this band shows the normal shift toward the singleton frequency of CO adsorbed on Pt.[27,29,46] The result demonstrates the complete segregation of the alloy due to oxidative treatment. The oxidation of Cu to Cu^{2+} and Cu^+ under these conditions could also be shown by XPS for the samples with the higher Cu loading.

4.3.2. Reduced Samples. Upon exposure to CO at elevated pressure the doublet at 2177 and 2150 cm^{-1} due to the Cu^+ dicarbonyl and following evacuation the narrow singlet at 2157 cm^{-1} due to the monocarbonyl can be clearly observed in all reduced samples (Figures 4−8) as was the case in all calcined samples. Sachtler et al. also observed mainly this band in Cu−ZSM-5 reduced even at 773 K.[30] The explanation is based on a general model developed by this group according to which Me^0 clusters (including Cu) are subjected to reoxidation by protons which is facilitated by CO.[47] The band of CO adsorbed atop metallic copper was also observed in the region at 2135−2121 cm^{-1}, but it was very unstable and easily removed under evacuation at ambient temperature. This is in agreement with literature data on Cu and Cu−Pt samples on other supports.[30,31]

The information on the modification of Pt by Cu and hence on alloying can be derived from the dynamic changes of the spectra during evacuation at ambient temperature and thermodesorption. The bands located between 2000 and 2100 cm^{-1} in the spectra definitely belong to CO atop Pt^0 in the metal clusters[27,29] and bands around 1878 cm^{-1} to bridge-bonded CO. The interpretation of the position of the bands in dependence on the Pt/Cu ratio of the samples and the observed shifts during desorption will be discussed in terms of geometric, electronic, and thermal effects.

As a general tendency, a decrease of the stretching vibration for CO atop bonded on Pt can be observed with increasing copper content. This is valid for the spectra following the evacuation of the samples at room temperature as well as for the position of the bands before complete desorption in the temperature program. The results are summarized in Table 3.

The observed spectra are indicative of alloy formation and show no signs of superimposed bands due to pure platinum particles, as for example found for Pt−Cr/H−ZSM-5.[29] The band positions of CO on top of pure Pt particles on the reoxidized sample 2 (0.6% Cu) can be used as a reference: 2086 cm^{-1} following evacuation (Figure 9a, spectrum 5) is typical for the blue shift due to dipole−dipole coupling;[48] 2061 cm^{-1} (Figure 9b, spectrum 6) can be assigned to the singleton frequency of the chemisorbed CO.[27] Bridge-bonded CO is hardly visible in the spectra. The result might indicate that at least in the case of samples 2 and 3 the singleton frequency is observed following exposure to CO and evacuation at room temperature, e.g., 2066 cm^{-1} (sample 2, Figure 6a, spectrum 4) and 2068 cm^{-1} (sample 3, Figure 8, spectrum 4), i.e., that the Pt surface is diluted by copper to the point where dipole−dipole coupling between the adsorbed CO molecules is absent or considerably reduced (geometric or ensemble effect). This is in agreement with Tolenaar et al.,[11] who could interpret similar shifts on the basis of a geometric effect alone.

TABLE 3: Summary of the Experimentally Observed CO Stretching Vibration in Dependence upon the Cu Content of the Reduced Samples

			band position (cm^{-1})		
sample	Cu (%)	reduction (K)	300 K[a]	423 K[b]	473 K[b]
1	2	523	2048	2041	2032
		623	2041	2033	
2	0.6	523	2066	2058	2052
		623	2060	2052	2045
3	0.3	523[c]	2064[c]		2055[c]
		623	2068		

[a] Following evacuation. [b] Following thermal desorption. [c] Reference 34.

Enrichment of the surface of the particles with the element with the lower heat of sublimation (Cu) can be expected.[49] This is in agreement with the results inferred from the EXAFS measurements for sample 2.[35] The further shift of the frequency of on-top adsorbed CO toward lower wavenumbers, i.e., 2055 cm^{-1} (sample 3[34]) and 2049 cm^{-1} (sample 2,Figure 6b, spectrum 6), at 473 K can then be attributed to the temperature-dependent downward shift of the frequency of the stretching vibration.[50]

An important observation in our samples is the observed tendency of a relative increase of CO adsorbed in the bridged position with increasing copper content. This can be seen in the case of sample 2 reduced at 623 K (1877 cm^{-1}, Figure 7a, spectrum 5) and most pronounced in the case of sample 1 with the highest copper content and reduced at 623 K (1878 cm^{-1}, Figure 5, spectrum 3). In the latter case even a reversal of the relative intensities bridged/atop in favor of the adsorption in the bridged position can be observed. It should be noted that the intensity of the signal due to linearly bonded CO has decreased considerably.

The experimental results can be interpreted in line with theoretical results[49,51] even though these were achieved for bulk metals or single-crystal surfaces.

The growing population of bridged sites with increasing copper content can be understood to be due to the contraction of the Pt d-band as a result of the incorporation of other atoms into the metal lattice.[52] Since chemisorption on a transition-metal surface involves interaction with the s,p- and d-valence electron band, an influence on the CO chemisorption bond type can be expected from a change of the d-band structure.[51,53] Considering the different symmetries of interaction, CO will preferentially occupy bridge positions if the interaction with a depleted d-valence electron band decreases.[51]

The observed red shift of the high-frequency band of CO atop Pt, which is most pronounced in the case of sample 1 with the highest copper content (2048 cm^{-1} following evacuation),

may also be caused by an electronic or ligand effect due to electron donation of the Cu to the Pt resulting in a stronger back-donation from the metal to the $2\pi^*$-orbital of the CO. A similar result has been reported in the case of Pt/Cr alloyed particles supported in H−ZSM-5.[29] A decrease of the frequency related to the size of the small metallic clusters as proposed in the literature[50] can be ruled out in the case of the alloyed particles.

While an exclusive electronic effect should merely increase the adsorption intensity for linearly bonded CO,[54,55] the observed actual decrease must be due to a diluted Pt surface. Nearly all the phenomena found here, i.e., decrease of the band intensity of linearly bonded CO for low degree of alloying or increase of the CO band intensity ratio bridged/linear with increasing degree of alloying, have recently been observed for the chemisorption of CO on Pt/Si alloys on a silica support.[56] They were interpreted by the operation of geometric and electronic effects as well.

5. Summary

Zeolite H−ZSM-5, ion-exchanged with $[Pt(NH_3)_4]^{2+}$ and Cu^{2+} in atomic ratios Cu/Pt between 1 and 6 and subsequently calcined in air, is studied with respect to the formation of Pt−Cu alloys upon reduction using X-ray photoelectron spectroscopy, Fourier transform infrared spectroscopy, and transmission electron microscopy. The electron micrographs reveal highly dispersed metal particles with narrow particle size distribution (1−2 nm) located within the zeolite host. Only a small number of larger metal aggregates (5−10 nm) can be found on the external surface of the zeolite carrier. All spectroscopic methods demonstrate the ready reoxidation and redispersion of the copper component in the alloyed particles.

The results obtained by TEM, XPS, and FTIR are clearly correlated. The most sensitive tool for detecting the alloy formation is the adsorption of CO. The results are explained on the basis of dominating electronic influences, where (1) a ligand effect leads to a stronger back-donation of electronic charge to the $2\pi^*$-orbital of the CO and (2) the narrowing of the Pt d-band in the alloy and the preferential interaction of the CO $2\pi^*$-orbital with the s-orbitals of the Pt surface results in an unusual high integral intensity for bridge-bonded CO. The additional geometric influence is due to the dilution of the Pt surface. Segregation of the alloy upon oxidation can be reversed by re-reduction.

Acknowledgment. We thank Dr. R. Lamber for providing the TEM data. The financial support by the Deutsche Forschungsgemeinschaft (438-113-139) and by INTAS (94-1402) is gratefully acknowledged.

References and Notes

(1) Sinfelt, J. H. *Bimetallic Catalysts*; Wiley: New York, 1983; p 86 ff.
(2) Ponec, V. *Adv. Catal*. **1983**, *32*, 149.
(3) Sachtler, W. M. H. *J. Mol. Catal*. **1984**, *25*, 1.
(4) Bond, G. F.; Yahya, R. *J. Chem. Soc., Faraday Trans. 1* **1991**, *87*, 775.
(5) Engstrom, J. R.; Goodman, D. W.; Weinberg, W. H. *J. Am. Chem. Soc.* **1986**, *108*, 4653.
(6) Shpiro, E. S.; Joyner, R. W.; Johnston, P.; Tuleuova, G. J. *J. Catal.* **1993**, *141*, 266.
(7) Naito, S.; Tanimoto, M. *J. Catal*. **1989**, *119*, 300.
(8) de Jongste, H. C.; Ponec, V.; Gault, F. G. *J. Catal*. **1980**, *63*, 395.
(9) de Jongste, H. C.; Ponec, V. *J. Catal*. **1980**, *63*, 389.
(10) Zholobenko, V. L.; Lei, G.-D.; Carvill, B. T.; Lerner, B. A.; Sachtler, W. M. H. *J. Chem. Soc., Faraday Trans.* **1994**, *90*, 233.
(11) Toolenaar, F. J. C. M.; Stoop, F.; Ponec, V. *J. Catal*. **1983**, *82*, 1.
(12) Stoop, F.; Toolenaar, F. J. C. M.; Ponec, V. *J. Catal.* **1982**, *73*, 50.
(13) Bastein, A. G. T. M.; Toolenaar, F. J. C. M.; Ponec, V. *J. Catal*. **1984**, *90*, 88.
(14) Toolenaar, F. J. C. M.; Reinalda, D.; Ponec, V. *J. Catal*. **1980**, *64*, 110.
(15) Rodriguez, J. A.; Campbell, R. A.; Goodman, D. W. *J. Phys. Chem.* **1991**, *95*, 5716.
(16) Rodriguez, J. A.; Goodman, D. W. *J. Phys. Chem*. **1991**, *95*, 4196.
(17) Moretti, G.; Sachtler, W. H. M. *J. Catal*. **1989**, *115*, 205.
(18) Tzou, M.-S.; Kusunoki, M.; Asakura, K.; Kuroda, H.; Moretti, G.; Sachtler, W. M. H. *J. Phys. Chem*. **1991**, *95*, 5210.
(19) Grünert, W.; Hayes, N. W.; Joyner, R. W.; Shpiro, E. S.; Siddiqui, M. R. H.; Baeva, G. N. *J. Phys. Chem*. **1994**, *98*, 10832.
(20) Iwamoto, M. *Stud. Surf. Sci. Catal*. **1990**, *54*, 121.
(21) Li, Y.; Hall, W. K. *J. Catal*. **1991**, *129*, 202.
(22) Montreuil, C. N.; Shelef, M. *Appl. Catal. B* **1992**, *1*, L1.
(23) Shelef, M. *Catal. Lett*. **1992**, *15*, 305.
(24) Petunchi, J. O.; Sill, G. A.; Hall, W. K. *Appl. Catal. B* **1993**, *2*, 303.
(25) Harkness, I. R.; Lambert, R. W. *J. Catal*. **1995**, *152*, 211.
(26) Hayes, N. W.; Grünert, W.; Hutchings, G. J.; Joyner, R. W.; Shpiro, E. S. *J. Chem. Soc., Chem. Commun.* **1994**, 531.
(27) Primet, M.; de Menorval, L.-C.; Fraissard, J.; Ito, T. *J. Chem. Soc., Faraday Trans. 1* **1995**, *81*, 2867.
(28) Shpiro, E. S.; Tkachenko, O. P.; Minachev, Kh. M. *Indian J. Technol*. **1992**, *30*, 161.
(29) Tkachenko, O. P.; Shpiro, E. S.; Jaeger, N. I.; Lamber, R.; Schulz-Ekloff, G.; Landmesser, H. *Catal. Lett*. **1994**, *23*, 251.
(30) Sarkany, J.; Sachtler, W. M. H. *Zeolites* **1994**, *14*, 7.
(31) Sarkany, J.; d'Itri, J. L.; Sachler, W. M. H. *Catal. Lett*. **1992**, *16*, 241.
(32) Joyner, R. W.; Shpiro, E. S.; Johnston, P.; Tuleuova, G. J. *J. Catal*. **1993**, *141*, 250.
(33) Minachev, Kh. M.; Shpiro, E. S. *The Catalyst Surface: Physical Methods of Studying*; MIR/CRC Press: Boca Raton, FL, 1990.
(34) Shpiro, E. S.; Jaeger, N. I.; Schulz-Ekloff, G. *Ber. Bunsen-Ges. Phys. Chem*. **1995**, *99*, 1321.
(35) Shpiro, E. S.; Joyner, R. W., unpublished results.
(36) Tong, Y.; Laub, D.; Schulz-Ekloff, G.; Renouprez, A. J.; van der Klink, J. J.; *Phys. Rev. B* **1995**, *52*, 8407.
(37) Clausen, B. S.; Gråbæk, L.; Topsøe, H.; Hansen, L. B.; Stoltze, P.; Nørskov, J. K.; Nielsen, O. H. *J. Catal*. **1993**, *141*, 368.
(38) Exner, D.; Jaeger, N. I.; Nowak, R.; Schulz-Ekloff, G.; Ryder, P. In *Proceedings of the 6th International Zeolite Conference*, 1983; Olson, D., Bisio, A., Eds.; Butterworths: Guildford, 1984; p 387. Exner, D.; Jaeger, N. I.; Kleine, A.; Schulz-Ekloff, G. *J. Chem. Soc., Faraday Trans. 1* **1988**, *84*, 4097. Tonscheidt, A.; Ryder, P. L.; Jaeger, N. I.; Schulz-Ekloff, G. *Surf. Sci.* **1993**, *281*, 51. Schulz-Ekloff, G.; Wright, D.; Grunze, M. *Zeolites* **1982**, *2*, 70. Schulz-Ekloff, G.; Jaeger, N. I. *Catal. Today* **1988**, *3*, 459. Rathousky, J.; Zukal, A.; Jaeger, N. I.; Schulz-Ekloff, G. *J. Chem. Soc., Faraday Trans.* **1992**, *88*, 489.
(39) Klier, K. *Langmuir* **1988**, *4*, 13. Ward, J. W. In *Zeolite Chemistry and Catalysis;* Rabo, J. A., Ed.; ACS Monograph, Vol. 171; American Chemical Society: Washington, DC, 1976; p 200.
(40) Miessner, H.; Landmesser, H.; Jaeger, N. I.; Richter, K. *J. Chem. Soc., Faraday Trans.* **1997**, *93*, 3417.
(41) Barshad, Y.; Zhou, X.; Gulari, E. *J. Catal*. **1985**, *94*, 128.
(42) Naccache, C.; Ben Taarit, Y. *J. Catal*. **1971**, *22*, 171.
(43) Piffer, R.; Hagelstein, M.; Cunis. S.; Rabe, P.; Förster, H.; Niemann, W. *Stud. Surf. Sci. Catal*. **1991**, *69*, 259.
(44) Bischoff, H.; Jaeger, N. I.; Schulz-Ekloff, G.; Kubelkova, L. *J. Mol.Catal.* **1993**, *80*, 95.
(45) Stakheev, A. Yu.; Shpiro, E. S.; Tkachenko, O. P.; Jaeger, N. I.; Schulz-Ekloff, G. *J. Catal.* **1997,** *169*, 382.
(46) Primet, M. *J. Catal*. **1984,** *88*, 273.
(47) Zhang, Z.; Xu, L.; Sachtler, W. M. H. *J. Catal*. **1991**, *131*, 502.
(48) Ertl, G.; Neumann, M.; Streit, K. M. *Surf. Sci*. **1977**, *64*, 393.
(49) van Santen, R. A.; Sachtler, W. M. H. *J. Catal*. **1974**, *33*, 202.
(50) Kappers, M. J.; Van der Maas, J. H. *Catal. Lett*. **1991**, *10*, 365.
(51) van Santen, R. A. *Recl. Trav. Chim. Pays-Bas* **1982**, *101*, 121.
(52) Siegel, E. *Semicond. Insul*. **1979**, *5*, 47.
(53) van Santen, R. A. *J. Chem. Soc., Faraday Trans*. **1987**, *83*, 1915.
(54) Rasband, B.; Hecker, W. C. *J. Catal*. **1993**, *139*, 551.
(55) Vannice, M. A.; Twu, C. C. *J. Chem. Phys*. **1981**, *75*, 5944.
(56) Hippe, C.; Lamber, R.; Schulz-Ekloff, G.; Schubert, U. *Catal. Lett*. **1997**, *47*, 195.